APPENDIX

The Slater integrals for the $(2p_{1/2}\,1g_{9/2})$ configuration are

$$F^k(2p,1g)\equiv\int\int u_{2p}{}^2(r_1)u_{1g}{}^2(r_2)f^k(r_1,r_2)r_1{}^2r_2{}^2dr_1dr_2,$$

$$G^k(2p,1g)\equiv\int\int u_{2p}(r_1)u_{2p}(r_2)u_{1g}(r_1)u_{1g}(r_2)\times f^k(r_1,r_2)r_1{}^2r_2{}^2dr_1dr_2.$$

$$F^0(2p,1g)=(1/3840)(385I_0+507I_1+1209I_2-501I_3+1899I_4-231I_5-1573I_6+2145I_7),$$

$$F^2(2p,1g)=(11/768)(35I_0+21I_1+15I_2-231I_3+249I_4+15I_5-299I_6+195I_7),$$

$$G^3(2p,1g)=(7/3840)(385I_0-811I_1+1289I_2-1707I_3+1867I_4-4169I_5+5291I_6-2145I_7),$$

$$G^5(2p,1g)=(121/3840)(35I_0-149I_1+415I_2-1065I_3+1865I_4-1855I_5+949I_6-195I_7).$$

PHYSICAL REVIEW VOLUME 115, NUMBER 6 SEPTEMBER 15, 1959

Elastic Scattering of N^{14} by Be^9

M. L. HALBERT AND A. ZUCKER
Oak Ridge National Laboratory, Oak Ridge, Tennessee*

(Received April 20, 1959)

Nitrogen-beryllium elastic scattering was measured over an angular range from 32 to 144 deg in the center-of-mass system with an angular resolution of about one degree. The mean energy of the incident nitrogen ions was 27.3 Mev. To distinguish elastic scattering from other events, both the scattered and the recoil particles were detected in coincidence by thin CsI(Tl) scintillation counters. The elastic scattering differential cross section is 550 mb/sterad at 32 deg c.m. It decreases monotonically and more rapidly than $\csc^4(\theta/2)$ to a shallow minimum of about 5 mb/sterad at 106 deg c.m., rises slightly, and then falls to about 2.5 mb/sterad at 144 deg c.m., the largest angle measured. The data are compared to the predictions of a sharp-cutoff model for elastic scattering, but no agreement is found between this theory and the experimental results.

INTRODUCTION

ELASTIC scattering is of considerable interest in the study of nuclear reactions and can be a useful tool for constructing nuclear potential models of all degrees of sophistication. Heavy-ion elastic scattering is susceptible to some simplifications because of the classical nature of the particles. The parameter $\eta=Z_1Z_2e^2/\hbar v$ indicates the degree to which a particle may be regarded as classical and is ordinarily larger than unity in heavy ion experiments.

Previously N^{14}—N^{14} elastic scattering was studied at this laboratory.[1] More recently, the elastic scattering angular distribution of C^{12} on Au^{197} was measured by Goldberg and Reynolds.[2] In both of these experiments it was found that the one free parameter of the semi-classical sharp-cutoff model proposed by Blair[3] can be chosen so that good agreement with the data is obtained. Theoretical considerations and experiments on elastic scattering of alpha particles from heavy elements[4] indicate that the Blair model provides a good fit if $\eta\gg1$, and $\sigma/\sigma_{\text{Coul}}>1/\eta$. Both heavy ion experiments cited above fulfill these requirements.

In the present measurement 27.8-Mev nitrogen-14 ions were scattered from beryllium. This corresponds to $\eta=3.2$, a value closer to unity than was encountered in previous experiments. Furthermore, it was found that over practically the entire angular region investigated $\sigma/\sigma_{\text{Coul}}<1/\eta$. Thus, although previous measurements of heavy-ion scattering lay in the domain of validity of the Blair model, it is not to be expected that this model will fit the results reported here.

DESIGN OF EXPERIMENT

In this experiment it was necessary to consider certain characteristics of 28-Mev nitrogen ions, the beryllium targets, and the kinematics of the scattering process in order to develop a workable design. Care had to be taken to avoid confusing nitrogen-beryllium elastic scattering with many possible similar events. These include inelastic scattering and transfer reactions[5] from beryllium and elastic scattering from impurities.

Self-supporting beryllium foils prepared by vacuum evaporation were used as targets. Typical thicknesses were about 0.18 mg/cm^2, representing approximately 1-Mev energy loss for the incident nitrogen beam.

Early in the course of this experiment it was found that the beryllium foils contained oxygen, and scattering from it competed seriously with the desired scattering. For example, at 20 deg laboratory angle the

* Operated for the U. S. Atomic Energy Commission by Union Carbide Corporation.

[1] H. L. Reynolds and A. Zucker, Phys. Rev. **102**, 1378 (1956).
[2] E. Goldberg and H. L. Reynolds, Phys. Rev. **112**, 1981 (1959).
[3] J. S. Blair, Phys. Rev. **95**, 1218 (1954).
[4] Wegener, Eisberg, and Igo, Phys. Rev. **99**, 825 (1955).
[5] Halbert, Handley, Pinajian, Webb, and Zucker, Phys. Rev. **106**, 251 (1957).

counting rate from oxygen was about equal to that from beryllium. Only a small percentage of target impurity is required for such a large effect, since (1) the oxygen is of higher atomic number than beryllium, (2) for the heavier oxygen atoms a given laboratory angle corresponds to a smaller center-of-mass angle, (3) the reduction in the scattering cross section due to nuclear effects is probably smaller for the oxygen since the energy is closer to the Coulomb barrier. There was no indication that other impurities were present in the targets, or accumulated on them during the course of the experiment.

Scattering from impurities can be distinguished from N−Be scattering if the detector has sufficiently good energy resolution. In this experiment, the detector was a Lucite-mounted 0.005-inch thick CsI(Tl) crystal[6] on a DuMont-6291 photomultiplier. Partly because of poor light-collection efficiency, its resolution was no better than about 10% for the most favorable particle energies. At forward angles this was inadequate to resolve nitrogen ions scattered by oxygen from nitrogen scattered by beryllium. Similarly, inelastic scattering from low-lying states or certain transfer reactions could not be cleanly separated from the elastic events.

The Coincidence Method

A reliable way of eliminating the unwanted counts is to take advantage of the differences in the kinematics for the various processes. For any choice of the N^{14} scattering angle, the angle at which the recoil particle is emitted during a given scattering process is known and may therefore be used to identify the process. In practice then the procedure was to detect either the nitrogen or beryllium atom in one scintillation counter, and to place a second counter at the proper angle to accept the other particle involved in the scattering event. Pulses from the first counter were displayed on a 20-channel pulse-height analyzer, which was gated by pulses from the second counter. In this way both coincidence and pulse-height information was obtained for each event. Figure 1 shows the kinematics of the elastic scattering.

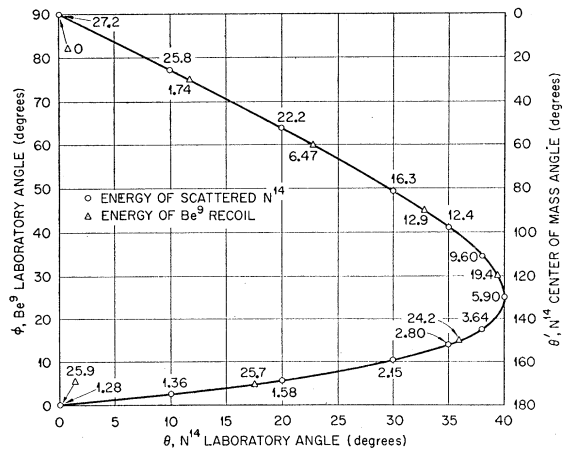

FIG. 1. Kinematics of the N^{14}-Be^9 elastic scattering for 27.2-Mev laboratory energy. Laboratory angles of both particles are given as a function of the nitrogen c.m. angle. Typical energies of nitrogen and beryllium at various angles are shown on the curve.

[6] Obtained from Isomet Corporation, Palisades Park, New Jersey.

An example of the usefulness of the coincidence method may be seen in Fig. 2 which shows nitrogen spectra taken at a laboratory angle of 20 deg. The impurity scattering peak is eliminated in the gated spectrum, and the low-energy continuum (probably due to reactions leading to multiparticle breakup) is also greatly reduced. The improvement is even more dramatic at larger angles, where the ungated spectrum usually shows no more than a slight bump at the pulse height expected for elastic scattering events.

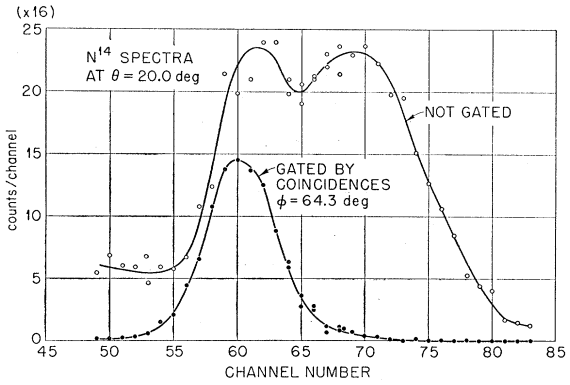

FIG. 2. Pulse-height distributions of counts in the defining counter gated and ungated by a second counter in coincidence. $\phi = 64.3$ deg is the laboratory angle at which Be recoils are expected for elastically scattered nitrogen detected at 20 deg in the laboratory system.

Figure 3 shows 20-deg spectra gated by the second counter at various angles. With this counter at 64.3 deg the peak is due to coincidences with recoil Be ions, as shown by the kinematics (Fig. 1). The asymmetric shape of the peak was probably caused by nonuniform scintillation response of the CsI crystal since the peak became symmetric with a smaller collimator in front of the crystal. The peak at the 70.3 deg position is probably N^{14} scattered by O^{16}. The energy ratio inferred from the two pulse heights[7] is just what one expects for nitrogen scattered from beryllium and oxygen, respectively. The area of the N−O peak is smaller than might be expected from the ungated spectrum of Fig. 2, probably because some of the O^{16} recoils were stopping in the target. Special care was taken, as described below, to avoid such losses in the scattering from Be.

In any such coincidence arrangement one must be

[7] M. L. Halbert, Phys. Rev. **107**, 647 (1957).

certain that the second counter accepts every particle associated with a desired particle entering the first counter. It is essential to know which counter is defining the angular acceptance of the coincidence system. The counter with the smaller aperture in the center-of-mass system will hereafter be called the *defining* counter, while the other will be referred to as the *conjugate* counter, in accordance with the nomenclature of Mather and Swan.[8] In estimating whether the conjugate aperture is sufficiently large, one must take into account the finite size of the beam spot and multiple scattering in the target. Whenever the latter effect might have been serious, experiments were conducted to insure that no counts were lost.

Accurate alignment of the counters is important. To prevent loss of coincidences the aperture of the conjugate counter must always remain in the plane determined by the incident beam direction and the defining aperture. By careful mechanical construction it was

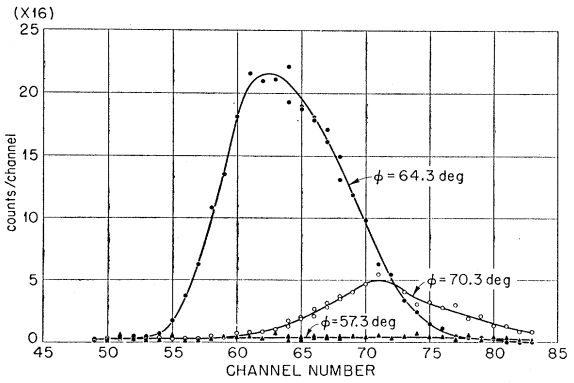

FIG. 3. Pulse-height distributions in the defining counter gated by the conjugate counter at various angles, ϕ, in the laboratory system.

assured that the plane of motion of the conjugate counter was parallel to that of the defining counter. To be certain that the planes actually coincided, a piece of paper masking tape was mounted over the aperture of each counter. The defining counter was moved into the direct beam and the orientation of the chamber was adjusted until the position of the charred spot on the tape indicated that the beam was striking at the center of that aperture. Then the conjugate counter was moved into the direct beam. The charred spot was found to be well-centered in the conjugate aperture, showing that the alignment was correct. This measurement was also used to determine the zero-degree setting of each counter. In a similar set of measurements with tape on the target holder, it was verified that the beam passed through the center of the chamber.

In spite of the coincidence technique, at certain

[8] K. B. Mather and P. Swan, *Nuclear Scattering* (Cambridge University Press, Cambridge, 1958), Chap. III.

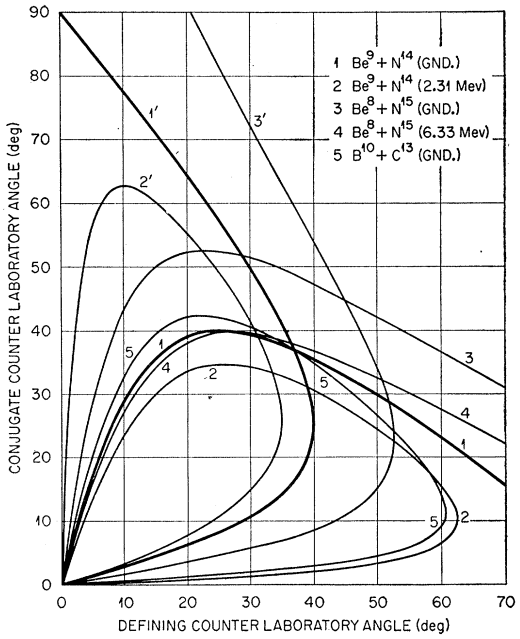

FIG. 4. Kinematics of some reactions which may be confused with elastic scattering events. The numbers identify the products of $N^{14}+Be^9$ reactions according to the legend in the diagram. Two curves are required for each reaction since either of the products may be counted in each detector. The primed curves give the required angle settings if the heavier product is to enter the defining counter. The unprimed curves are for the inverse case.

angles confusion with unwanted events was possible. Figure 4 shows how this may arise. For simplicity only a few of the possible reactions are shown.[9] The curves identified by primed numbers are those in which the heavier particle enters the defining counter; the unprimed curves describe the opposite situation. The points where these curves cross the elastic scattering curves (1 and 1′) then give the angle settings at which confusion may occur. At nearly all intersections of the elastic scattering curves with the other primed and unprimed curves the pulse height in the defining counter was quite different for the two processes and a clear distinction was easily made. However, where curve 1 crosses curve 5 the particle energies differ by only about 10%, and a clean separation of the Be^9 from the B^{10} could not be expected. From the shape of the spectra obtained at these angles (128 to 132 deg c.m.) there was no evidence for any B^{10} pulses. The data were analyzed on the assumption that all counts were due to Be^9.

The reactions leading to Be^8 deserve special mention. By virtue of the transverse momentum which may be

[9] So many reactions may occur that hand calculation of the kinematics becomes exceedingly time-consuming. A program for the IBM-704 computer was developed to calculate certain kinematic quantities for nonrelativistic reactions resulting in two particles. The machine prints out the following information for each reaction product as a function of the center-of-mass angle: (a) laboratory angle, (b) laboratory energy, (c) solid-angle transformation from laboratory to c.m. system, (d) time of flight in nanoseconds/meter (10^{-9} sec/meter), and (e) magnetic rigidity.

imparted to the alpha particles produced when the Be^8 breaks up, one of them might be detected even if the counters are not at the correct angles for (Be^8+N^{15}) detection. In most situations of interest in this experiment, the Be^8 kinetic energy is large compared with its distintegration energy. The maximum angle between the alpha-particle direction and the initial Be^8 direction is therefore only a few degrees, and most of the alpha particles do not deviate even this much from the initial direction. By broadening the appropriate lines in Fig. 4 to represent the maximum possible deviation of the alpha particles from the Be^8 angle of emission, it can be shown that of the reactions leading to Be^8 in its ground state only those resulting in N^{15} excited to the 6.33 Mev (curve 4) or higher states might be mistaken for elastic scattering events. Fortunately, the Be^9 pulse height is sufficiently different from that of the alpha particle to permit a good separation.

The Scattering Chamber

Figure 5 is a simplified diagram of the scattering chamber. Its interior diameter is 24 inches and its depth about 8 inches. Each counter and its associated magnetic shielding is mounted on a rigid aluminum arm whose angle can be changed manually from outside the chamber. A worm-gear drive for each counter with a 100-to-1 reduction makes it possible to move the heavy iron shielding against the magnetic forces and also provides a brake against the pull of the field on the counters.

The counter arms are mounted on concentric shafts with rotating O-ring seals and can be moved independently of each other. A stationary tube inside the smaller shaft provides support for the target-carrying rod and an unobstructed annulus for electrical connections. The target can be positioned in and out of the incident beam and be rotated on the axis of the counter motion. These adjustments can be made without breaking the vacuum.

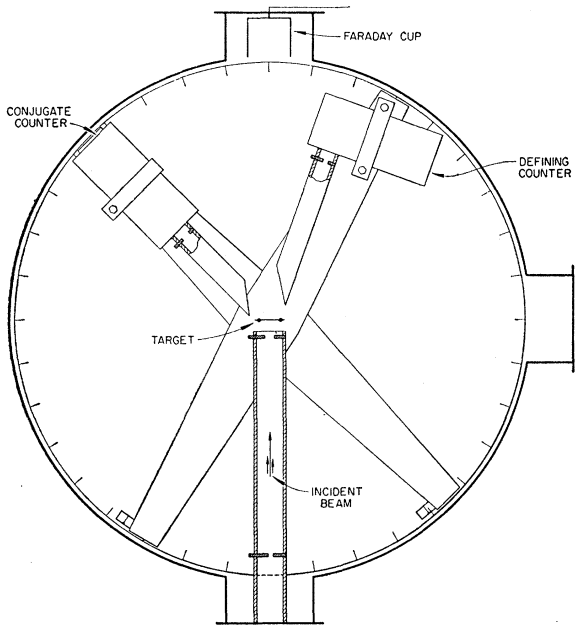

FIG. 5. Schematic drawing of the scattering chamber.

All mechanical support and electrical connections are thus provided through one wall of the chamber. The opposite wall of the chamber is a 2-inch thick, 27.5-inch diameter laminated glass disk. Through it the entire interior of the chamber can be seen. This feature proved its worth many times. The location and condition of the target, the electrical leads, the collimators, and the counters can all be checked at a glance or adjusted easily. An angle scale engraved on the inner face of the supporting wall is also easily visible. By means of a reference marker attached to each arm, the counter angles can be reproducibly set to ± 0.1 deg.

Access to the inside of the chamber is provided by three 4.5-inch diameter ports. One serves as the beam entrance port, another is opposite the entrance port, and the third is at 90 deg to the incident beam direction.

The scattering chamber was located near the cyclotron, in a fringing field of about 1000 gauss near the entrance collimator and decreasing to several hundred gauss at the defining counter. Each photomultiplier was shielded simply and effectively with a close-fitting mu-metal cylinder and two concentric iron cylinders. The effect of the magnetic field on the particle trajectories constituted a serious problem, particularly when it was necessary to detect low-energy particles. To minimize curvature of the paths and separation of the charge states, the particles traveled inside an iron pipe installed on each counter between the target position and the counter aperture. A third pipe was used to shield the path of the incident beam before it reached the target.

All apertures were circular. The entering N^{14} beam was collimated by a $\frac{1}{8}$-inch diameter hole $10\frac{3}{4}$ inches from the target. The beam was slightly divergent; when it reached the target it was at most $\frac{5}{32}$ inch in diameter. The divergence of the beam was thus no larger than ± 0.1 deg.

The collimator of the defining counter was either $\frac{1}{8}$ inch or $\frac{1}{16}$ inch in diameter depending on the experimental requirements. Located $7\frac{3}{8}$ inches from the center of the chamber, these collimators subtended a cone of half angle slightly less than 0.5 deg or 0.25 deg. The true angular resolution was somewhat larger, due to factors such as the finite beam size and multiple scattering.

The conjugate counter was normally used with a $\frac{3}{8}$-inch diameter aperture placed about $3\frac{3}{4}$ inches from the center of the chamber so that it subtended a cone of half angle approximately 2.9 deg. The size of the collimator could be varied for experimental checks of multiple scattering effects.

EXPERIMENTAL PROCEDURE

The electronic apparatus for this experiment was fairly standard. Pulses from the two scintillation counters passed through cathode followers and were amplified by linear amplifiers. An integral discriminator following the conjugate-counter amplifier was used to gate a 20-channel pulse-height analyzer on which the pulses from the defining counter were displayed. The resolving time of the circuit was about 2.8 μsec.

As mentioned previously, the coincidence method requires that one take special care to be sure that no counts are lost. Experimental tests were devised to check that: (a) the conjugate counter was at the proper angle, (b) all coincident particles had sufficient energy to leave the target and be detected by the conjugate counter, (c) the aperture of the conjugate counter was large enough to accept all coincident particles, and (d) all coincident particles entering the conjugate counter actually gated the pulse-height analyzer.

To check (a) and (c), the coincidence rate for a given setting of the defining counter was measured as a function of the conjugate-counter position. Figure 6 shows such a curve with the defining counter at 20 deg. The expected angle for detection of recoil Be particles is 64 deg. The curve immediately checks condition (a), while the existence of a plateau is evidence that requirement (c) is satisfied. A similar curve was obtained for every setting of the defining counter.

If a good plateau was not obtained it was usually because coincident particles were multiply scattered as they passed out of the target. Tilting the target so that these particles traversed a shorter length of target material would in most cases restore the flat top. When this failed to give a good plateau, a direct check on multiple scattering was made. The usual $\frac{3}{8}$-inch diameter collimator on the conjugate counter was replaced by a $\frac{5}{16}$-inch collimator. If no reduction in coincidence rate was observed, the $\frac{3}{8}$-inch collimator

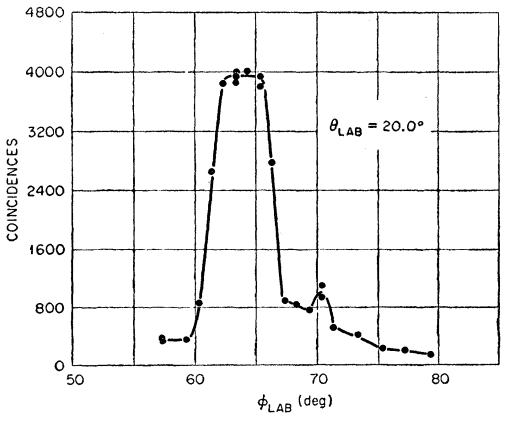

FIG. 6. Coincidence rate as a function of conjugate counter angle, ϕ. The defining counter was fixed at 20 deg in the laboratory system. The small peak at 70 deg is probably due to oxygen impurity in the target.

was clearly large enough to satisfy (c). On the other hand, if a counting loss was observed the data at this angle were not used for a cross-section determination. This condition limited the smallest angle to 12.5 deg, laboratory system. A larger aperture on the conjugate counter might have permitted additional measurements, but other difficulties with the low-energy recoils would have precluded their extension to angles significantly smaller than 12.5 deg.

The pulse-height analyzer was gated by pulses in the conjugate counter above a certain threshold. To check (b) and (d) the coincidence rate was measured as a function of this threshold setting. Ordinarily the curve obtained showed a broad region in which the coincidence rate was independent of pulse-height setting. This was taken as sufficient evidence that (b) and (d) were satisfied. If the coincident particle was of low energy the curve tended to have a shorter plateau. In such cases tilting the target toward the conjugate counter lengthened the plateau. However, at no angle permitted by requirement (c) was there any doubt that all the coincident particles were reaching the conjugate counter and turning on the gate circuit.

For the cross-section measurements from 32 deg c.m. to 90 deg c.m., the defining counter was used to detect the scattered N^{14}. Near 90 deg c.m., however, several difficulties manifested themselves. (1) Background in the gated spectra became a problem. As the large-aperture conjugate counter was moving further forward many more gate openings not due to the desired elastic scattering events occurred. (2) The defining aperture corresponded to a very large angular acceptance in the center-of-mass system. (3) Multiple scattering of the N^{14} became appreciable. The last two effects tended to decrease the effective angular resolution.

All of the above difficulties were alleviated simply by interchanging the roles of the counters. That is, the Be^9 recoils entered the defining counter while the coincident N^{14} ions were detected by the conjugate counter. Eventually, however, as the measurements were extended to much larger angles, the decreasing cross section and increasing background combined to make the data uncertain. For example, at the largest angle studied (144 deg c.m.) the uncertainty in subtraction of the background continuum was of the order of 20%.

In an attempt to study the origin of the background, a pair of large-angle runs was taken with full beam intensity and with one-fourth of full beam. The two runs gave identical spectra. This showed that the background was not due to random coincidences, but to real nonscattering events. These may have been many-body disintegrations in which two of the charged reaction products happened to enter the counters. The angular distribution was not extended beyond 144 deg since the background would have been extremely difficult to eliminate, and it was likely that multiple scattering losses due to the low energy of the N^{14} ions

would have prevented measurements at angles not much larger than 144 deg. Furthermore, at these angles the counting rate in the conjugate counter was highest and therefore the pair of runs at high and low beam level showed that the contribution of chance coincidences to the elastic scattering peak was negligible, as was blocking of the gating circuit by a high counting rate.

To measure the scattering cross section it is necessary to know the number of nitrogen ions striking the target per unit time. This was done by measuring and integrating the beam current after it passed through the target. An insulated cover plate on the forward port was used for this purpose. A check with a Faraday cup showed that no errors in these measurements were caused by escape of secondary electrons.

To check for proper overall operation of the detection system and also for possible vaporization of target material, frequent runs were made at certain standard angles, at least once every three hours. These standard angles (66.1 deg c.m. when the N^{14} was detected by the defining counter and 85 deg c.m. when the Be^9 entered this counter) were selected for their high counting rates and the absence of the experimental difficulties described above. It was found that these runs for a given target were consistent within the statistical error.

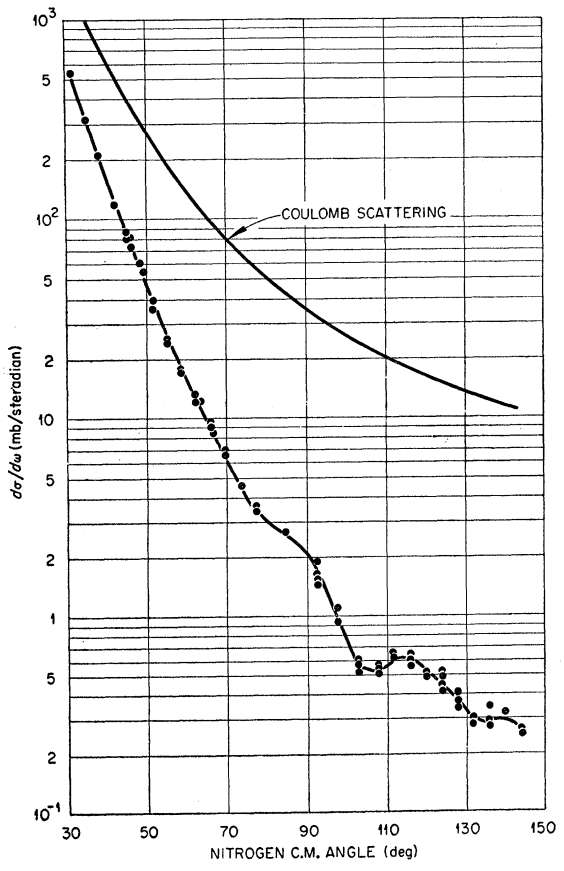

FIG. 7. The differential cross section of N^{14}—Be^9 elastic scattering as a function of the nitrogen c.m. angle. All experimental points are shown except at 85 deg where many points were taken and only an average is shown. The upper curve is the cross section for Coulomb scattering.

The energy of the beam was determined by placing a hydrogen-filled chamber at the forward port of the scattering chamber, and measuring the range in emulsion of recoil protons at zero degrees. This method has been described in detail previously.[10] No continuous check on the beam energy during the scattering was made; however, past experience indicates that the beam energy was probably constant to within ±200 kev. Since the targets were relatively thick, usually about 1 Mev, no effects due to small beam-energy fluctuations could have been observed. All cross-section calculations are based on a mean energy in the target of 27.3 Mev.

RESULTS

We present the results of this experiment graphically in Fig. 7. All acceptable experimental points are shown in this figure. The angular resolution in the center-of-mass system was about one degree up to 77 deg, and somewhat larger beyond this angle. We also show for comparison the differential cross section for Coulomb scattering calculated from the relation $d\sigma_{\text{Coul}}/d\omega = (Z_1Z_2e^2/2\mu v^2)^2 \csc^4(\theta/2)$. Here μ is the reduced mass, v the relative velocity, and θ the angle of scatter of the N^{14} in the center-of-mass system.

The results are also presented in tabular form for the convenience of those who might want to analyze the data further. Table I gives the elastic-scattering differential cross section and its ratio to the Coulomb cross section. The percent errors listed are estimates of the standard deviation and include such effects as statistical fluctuations, uncertainties in background subtraction, errors in angle setting, and random errors in beam integration. At large angles the increased error is due mainly to uncertainties in background subtraction.

The measured cross section in the region from 128 to 132 deg c.m. may be too large because of the previously mentioned confusion with the reaction $Be^9(N^{14},B^{10})C^{13}$. We estimate that the contribution of this transfer reaction is probably not larger than 40%.

Systematic Errors

In addition to the relative errors listed in Table I, there are systematic errors which do not change the shape of the angular distribution but do affect the absolute value of the cross section. These errors arise from uncertainties in (1) the target thickness, purity, uniformity and tilt; (2) the solid angle subtended by the defining counter; (3) the average charge of nitrogen ions emerging from the target; and (4) the beam-

[10] Reynolds, Scott, and Zucker, Phys. Rev. **102**, 237 (1956).

integrator calibration. All percent errors given below are estimated standard deviations.

The target thickness was determined by weighing the beryllium foils and measuring their area. These measurements were subject to an error estimated to be $\pm 10\%$. Appreciable oxygen contamination was present in the foils, and the weight of oxygen had to be subtracted from the gross foil weight. The amount of oxygen in one target was estimated in the following way. From the ungated spectrum at 20 deg lab (Fig. 2), the relative number of nitrogen ions scattered by oxygen and beryllium was determined. The N−O elastic cross section at this angle was estimated to be three quarters of the Coulomb cross section. This number is probably accurate to 30%. The total percentage of oxygen in the target calculated on this basis is 7.4 ± 2.2 by weight. The same figure was used to correct the weight of the other targets.

The uniformity of the targets is more difficult to evaluate. No measurable difference in the counting rate was found when various portions of a foil were used, and data from four different targets, when normalized to the same target weight, gave the same results. The effect of nonuniformity is thus probably small compared to the 10% standard deviation due to the thickness measurements themselves. The target tilt which was necessary for small and large angle measurements produced an additional uncertainty of 3%.

The solid angle subtended by the defining aperture, computed from its diameter and its distance from the target, could have been in error by about 4%. The average charge was calculated from the equilibrium charge distribution for nitrogen in plastic foils.[11] It also might have been in error by several percent. The absolute calibration of the beam integrator was uncertain by a similar amount. Fortunately these three uncertainties may be eliminated by measuring the counting rate for some process with a known cross section from a target of accurately known thickness. In effect one substitutes one error, that in the thickness of this secondary target, for the three uncertainties given above.

The process chosen for the absolute calibration was elastic scattering of nitrogen from a thin nickel foil. The available nitrogen energy is well below the Coulomb barrier for nickel, and the scattering cross section can therefore be readily calculated. It was found that over the entire range of defining counter settings used in the nickel scattering the cross section exhibits the expected $\csc^4(\theta/2)$ shape, thus providing a check on the measured laboratory angles. The N−Be absolute differential cross section calculated from the measured solid angle, estimated average charge of the beam, and integrator calibration agreed with the cross section based on the nickel calibration to within 2%.

The uncertainty in the nickel thickness measurement was $\pm 3\%$. The root-mean-square error from all systematic factors was thus about $\pm 11\%$, due mostly to the uncertainty in the Be target thickness.

TABLE I. Differential cross section for N^{14}-Be^9 elastic scattering and its ratio to Coulomb scattering at 27.3-Mev incident nitrogen energy.

Nitrogen center-of-mass angle (degrees)	$d\sigma/d\omega_{c.m.}$ (mb/sterad.)	Standard deviation[a] (percent)	$d\sigma/d\sigma_{Coul}$
32.2	551	5	0.366
35.5	317	5	0.308
38.7	213	5	0.290
42.2	119	5	0.224
45.4	81.1	5	0.202
48.9	61.2	5	0.202
52.1	39.8	5	0.166
55.7	25.5	5	0.137
59.0	15.4	5	0.116
62.7	12.7	5	0.104
66.1	9.67	5	0.0961
69.9	6.79	5	0.0812
74.0	4.59	5	0.0676
77.3	3.51	5	0.0602
85.0	2.71	5	0.0634
93.0	1.64	8	0.0508
98.0	1.03	10	0.0374
103.0	0.571	8	0.0241
108.0	0.537	6	0.0259
112.0	0.640	6	0.0340
116.0	0.610	10	0.0354
120.0	0.502	10	0.0317
124.0	0.460	10	0.0314
128.0	0.378	10	0.0277
132.0	0.284	15	0.0223
136.0	0.293	20	0.0243
140.0	0.323	20	0.0283
144.0	0.254	20	0.0233

[a] The standard deviation is for random errors only. For systematic errors see text.

Inelastic Scattering

The cross section for inelastic scattering to the 2.31-Mev state in N^{14} was measured at 66 deg and 98 deg c.m. At 66 deg a peak for this process was found and the cross section is 0.04 ± 0.01 mb/sterad. At 98 deg no inelastic peak was found, and an upper limit to the cross section is 0.005 mb/sterad.

DISCUSSION

The sharp-cutoff model proposed by Blair for elastic scattering postulates that the scattering nucleus absorbs completely all partial waves from $l=0$ to a certain cutoff l-value, while all the partial waves with $l > l_{cutoff}$ are Coulomb-scattered. This model has shown good agreement with data from elastic scattering of alpha particles by heavy nuclei[4] provided $\eta = Z_1 Z_2 e^2/\hbar v$ is large compared to unity and if $\sigma/\sigma_{Coul} > 1/\eta$. In the two experiments cited in the introduction both these conditions hold: in the $N^{14}-N^{14}$ scattering, $\eta = 6.1$ and σ/σ_{Coul} was always greater than $\frac{1}{4}$, while in the nitrogen-gold scattering η varied from 24.5 to 31.0, and the

[11] Reynolds, Wyly, and Zucker, Phys. Rev. 98, 474 (1955).

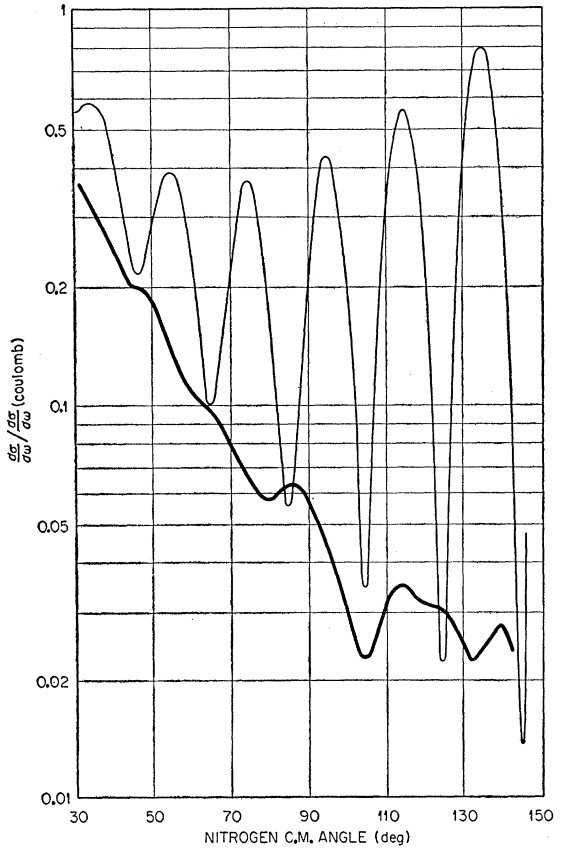

FIG. 8. The heavy curve represents the elastic cross section divided by the Coulomb cross section. The lighter oscillating curve is the result of a sharp-cutoff calculation using $l_{\max}=8$.

experimental measurements were limited to the angular region where $\sigma/\sigma_{\text{Coul}}>\frac{1}{10}$.

In this experiment, however, $\eta=3.2$, and $\sigma/\sigma_{\text{Coul}}<1/3.2$ over the entire measured portion of the angular distribution. Hence one should not expect the sharp-cutoff theory to agree with the experimental results.

The heavy line in Fig. 8 is the ratio of the experimental cross section to the Coulomb cross section, and the rapidly oscillating lighter curve is calculated from the Blair model according to the formula

$$\frac{d\sigma}{d\omega}=\left|\frac{-\eta}{2k\sin^2(\theta/2)}\exp[-i\eta\ln\sin^2(\theta/2)]e^{2i\delta_0}-\frac{1}{2ik}\sum_{l=0}^{8}(2l+1)e^{2i\delta_l}P_l(\cos\theta)\right|^2,$$

where θ is the c.m. angle, k is the wave number of the relative motion, and $\delta_l=\Gamma(l+1+i\eta)/\Gamma(l+1-i\eta)$. The cutoff l-value of 8 was obtained from the semiclassical relation

$$l(l+1)\hbar^2=2\mu R^2(E-E_B),$$

where μ=reduced mass, E=center-of-mass energy, $E_B=Z_1Z_2e^2/R$, and $R=1.5(A_1^{\frac{1}{3}}+A_2^{\frac{1}{3}})$ fermis. Calculations using cutoff l-values of 6, 7, 9, and 10 were also made and show no better agreement with the data.

No further attempt has been made to interpret the results of the present experiment. Other approaches, such as a phase-shift analysis or complete optical-model calculation may well provide valuable information about the behavior of nuclei in close collision. Such calculations are, however, beyond the scope of this work.

ACKNOWLEDGMENTS

The authors wish to thank J. A. Northrop for kindly providing the precious beryllium foils. We are indebted to H. L. Reynolds, and E. Goldberg who made the IBM-650 code for the Blair model calculation available, and to B. D. Williams who developed the kinematics program for the IBM 704. Our thanks go also to J. G. Harris for the construction of a large part of the apparatus, to A. W. Riikola and H. L. Dickerson for their untiring efforts in operating the cyclotron, and to C. E. Hunting and G. A. Palmer for their valuable assistance in taking data.